Simultaneous Selection of Multiple Important Single Nucleotide Polymorphisms in Familial Genome Wide Association Studies Data

Subhabrata Majumdar[*], University of Florida
Saonli Basu and Snigdhansu Chatterjee[†], University of Minnesota Twin Cities

Abstract

We propose a resampling-based fast variable selection technique for selecting important Single Nucleotide Polymorphisms (SNP) in multi-marker mixed effect models used in twin studies. Due to computational complexity, current practice includes testing the effect of one SNP at a time, commonly termed as 'single SNP association analysis'. Joint modeling of genetic variants within a gene or pathway may have better power to detect the relevant genetic variants, hence we adapt our recently proposed framework of e-values to address this. In this paper, we propose a computationally efficient approach for single SNP detection in families while utilizing information on multiple SNPs simultaneously. We achieve this through improvements in two aspects. First, unlike other model selection techniques, our method only requires training a model with all possible predictors. Second, we utilize a fast and scalable bootstrap procedure that only requires Monte-Carlo sampling to obtain bootstrapped copies of the estimated vector of coefficients. Using this bootstrap sample, we obtain the e-value for each SNP, and select SNPs having e-values below a threshold. We illustrate through numerical studies that our method is more effective in detecting SNPs associated with a trait than either single-marker analysis using family data or model selection methods that ignore the familial dependency structure. We also use the e-values to perform gene-level analysis in nuclear families and detect several SNPs that have been implicated to be associated with alcohol consumption.

Keywords: Family data; Twin studies; ACE model; Model selection; Resampling; Generalized bootstrap

[*]The author acknowledges the University of Minnesota Interdisciplinary Doctoral Fellowship program.
[†]Partially supported by the National Science Foundation (NSF) under grants # DMS-1622483, # DMS-1737918.

1 Introduction

Genome Wide Association Studies (GWAS) have identified a large number of genetic variants associated with complex diseases (Chang et al., 2014; Wheeler and Barroso, 2011). The advent of economical high-throughput genotyping technology enables researchers to scan the genome with millions of SNPs, and improvements in computational efficiency in analysis techniques has facilitated parsing through this huge amount of data to detect significant associations (Visscher et al., 2012). Detecting small effects of individual SNPs requires large sample size (Manolio et al., 2009), which is a major challenge of these studies. For quantitative behavioral traits such as alcohol consumption, drug abuse, anorexia and depression, variation in genetic effects due to environmental heterogeneity brings in additional noise, further amplifying the issue. This is one of the motivations of performing GWAS on families instead of unrelated individuals, through which the environmental variation can be reduced (Benyamin et al., 2009; Miller et al., 2012; Visscher et al., 2017). However, association analysis using families can be computationally very challenging and thus single SNP association analysis is the standard tool for detecting SNPs. The Minnesota Twin Family Study (Miller et al., 2012) with genome-wide data on identical twins, non-identical twins, biological offsprings, adoptees serve as the motivation for our methodology development in this paper.

Single-SNP analysis tests for association between the trait and a single SNP at a time. The SNPs with p-values lower than a particular threshold are considered to be associated with the trait. The GRAMMAR method of Aulchenko et al. (2007) and the association test of Chen and Abecasis (2007) are examples of such techniques applied to familial data. While they can efficiently analyze GWAS data, they assume that phenotypic similarity within families is entirely due to their genetic similarity and ignore the effect of shared environment. As a result, they tend to lose power when analyzing data where shared environmental effects explain a substantial proportion of the total phenotypic variation (see McGue et al. (2013) and De Neve et al. (2013) for example). In contrast, the RFGLS method proposed by Li et al. (2011) takes into account genetic and environmental sources of familial similarity and still provides fast inference through a rapid approximation of the single-SNP mixed effect model.

Single-SNP methods are prone to be less effective in detecting SNPs with weak signals (Manolio et al., 2009). This includes instances where multiple SNPs are jointly associated with the phenotype (Yang et al., 2012; Ke, 2012; Schifano et al., 2012). Several methods of multi-SNP analysis have been proposed as alternatives. The kernel based association tests (Schifano et al., 2012; Chen et al., 2013; Schaid et al., 2013; Ionita-Laza et al., 2013) are prominent among such techniques. However, all of them test for whether a *group* of SNPs is associated with the phenotype being analyzed, and do not generally prioritize within the group and detect the individual SNPs primarily associated with the trait.

One way to solve this problem is to perform model selection. The methods of Frommelet et al. (2012) and Zhang et al. (2014) take this approach, and perform SNP selection from a multi-SNP model on GWAS data from *unrelated individuals*. However, they rely

on fitting models corresponding to multiple predictor sets, hence are computationally very intensive to implement in a linear mixed-effect framework for modeling familial data.

In this paper we propose a fast and scalable model selection technique thats fits a single model to a family data, and aims to identify important genetic variants with weak signals through joint modelling of multiple variants. We consider only main effects of the variants, but this can be extended to include higher-order interactions. We achieve this by extending the recently proposed framework of e-values (Majumdar and Chatterjee, 2017). For any estimation method that provides consistent estimates (at a certain rate relative to the sample size) of the vector of parameters, e-values quantify the proximity of the sampling distribution for a restricted parameter estimate to that of the full model estimate in a regression-like setup. A variable selection algorithm using the e-values has the following simple and generic steps:

1. Fit the full model, i.e. where all predictor effects are being estimated from the data, and use resampling to estimate its e-value;

2. Set an element of the full model coefficient estimate to 0 and get an e-value for that predictor using resampling distribution of previously estimated parameters- repeat this for all predictors;

3. Select predictors that have e-values below a pre-determined threshold.

The above algorithm offers multiple important benefits in the SNP selection scenario. Unlike other model selection methods, only the full model needs to be computed here. It thus offers the user more flexibility in utilizing a suitable method of estimation for the full model. Our method allows for fitting multi-SNP models, thereby accommodating cases of modelling multiple correlated SNPs or closely located multiple causal SNPs simultaneously. Finally, we use the Generalized Bootstrap (Chatterjee and Bose, 2005) as our chosen resampling technique. Instead of fitting a separate model for each bootstrap sample, it computes bootstrap estimates using Monte-Carlo samples from the resampling distribution as weights, and reusing model objects obtained from the full model. Consequently, the resampling step becomes very fast and parallelizable.

The rest of the paper is organized as follows. Section 2 provides background information on the GWAS Family dataset we use in our case study, as well as introduces the statistical framework we use to model this data. We start Section 3 by providing a technical introduction to the e-values framework, then elaborate on the necessary modifications for adapting it to our modelling scenario, and present details of the bootstrap procedure. We illustrate the performance of this method on synthetic datasets in Section 4. In Section C we analyze our GWAS dataset using the e-values technique to identify novel SNPs from multiple genes that have been reported to influence alcohol consumption in individuals. Finally in Section 6 we outline directions of future research. We include the proofs of all new results stated, specifically, theorems 3.2 and 3.3, in the supplementary material.

2 Data and model

2.1 The MCTFR data

The familial GWAS dataset collected and studied by Minnesota Center for Twin and Family Research (MCTFR)(Li et al., 2011; Miller et al., 2012; McGue et al., 2013) consists of samples from three longitudinal studies conducted by the MCTFR: (1) the Minnesota Twin Family Study (MTFS: Iacono et al. (1999)) that covers twins and their parents, (2) the Sibling Interaction and Behavior Study (SIBS: McGue et al. (2007)) that includes adopted and biological sibling pairs and their parents, and (3) the enrichment study (ES: Keyes et al. (2009)) that extended the MTFS by oversampling 11 year old twins who are highly likely to develop substance abuse. While 9827 individuals completed the initial assessments for participation in the study, after several steps of screening (Miller et al., 2012) the final sample consisted of 7605 Caucasian individuals clustered in 2151 nuclear families. This consisted of 1109 families where the children are identical twins, 577 families with non-identical twins, 210 familes with adopted children, 162 families with non-twin biological siblings, and 93 families wher one child is adopted while the other is the biological child of the parents.

DNA samples collected from the subjects were analyzed using Illumina's Human660W-Quad Array, and after standard quality control steps (Miller et al., 2012), 527,829 SNPs were retained. Covariates for each sample included age, sex, birth year, generation (parent or offspring), as well as two-way interactions between generation and other three covariates each. Five quantitative phenotypes measuring substance use disorders were studied in this GWAS: (1) Nicotine dependence, (2) Alcohol consumption, (3) Alcohol dependence, (4) Illegal drug usage, and (5) Behavioral disinhibition. The response variables corresponding to these phenotypes are derived from questionnaires using a hierarchical approach based on factor analysis (Hicks et al., 2011).

A detailed description of the data is available in Miller et al. (2012). Several studies reported SNPs associated with phenotypes collected in MCTFR study (Li et al., 2011; McGue et al., 2013; Coombes et al., 2017). Li et al. (2011) used RFGLS to detect association between height and genetic variants through single-SNP analysis, while McGue et al. (2013) used the same method to study SNPs influencing the development of all five indicators of behavioral disinhibition mentioned above. Irons (2012) focused on the effect of several factors affecting alcohol use in the study population, namely the effects of polymorphisms in the ALDH2 gene and the GABA system genes, as well as the effect of early exposure to alcohols as adolescents to adult outcomes. Finally Coombes et al. (2017) used a bootstrap-based combination test and a sequential score test to evaluate gene-environment interactions for alcohol consumption.

2.2 Statistical model

We use a Linear Mixed Model (LMM) with three variance components accounting for several potential sources of variation to model effect of SNPs behind a quantitative phe-

notype. This is known as *ACE model* in the literature (Kohler et al., 2011). While the-state-of-the-art focuses on detection of a *single variant at a time*, we will incorporate *all* SNPs genotyped within a gene (or group of genes in some cases) as set of fixed effects in a *single model*.

Our model fitting process is invariant to pedigree sizes. In the present context we assume nuclear pedigrees, as previously implemented by Chen and Abecasis (2007); Li et al. (2011); McGue et al. (2013). Suppose there are m families in total, with the i^{th} pedigree containing n_i individuals. Denote by $y_i = (y_{i1}, \ldots, y_{in_i})^T$ the quantitative trait values for individuals in that pedigree, while the matrix $\mathbf{G}_i \in \mathbb{R}^{n_i \times p_g}$ contains their genotypes for a number of SNPs. Let $\mathbf{C}_i \in \mathbb{R}^{n_i \times p}$ denote the data on p covariates for individuals in the pedigree i. Given these, we consider the following model.

$$\mathbf{Y}_i = \alpha + \mathbf{G}_i\beta_g + \mathbf{C}_i\beta_c + \epsilon_i \tag{2.1}$$

with α the intercept term, β_g and β_c fixed coefficient terms corresponding to the multiple SNPs and covariates, respectively, and $\epsilon_i \sim \mathcal{N}_{n_i}(\mathbf{0}, \mathbf{V}_i)$ the random error term. To account for the within-family dependency structure, we break up the random error variance into three independent components:

$$\mathbf{V}_i = \sigma_a^2\mathbf{\Phi}_i + \sigma_c^2\mathbf{1}\mathbf{1}^T + \sigma_e^2\mathbf{I}_{n_i} \tag{2.2}$$

The first component above is a within-family random effect term to account for polygenic effects. The matrix $\mathbf{\Phi}_i$ is the relationship matrix within the i^{th} pedigree. Its $(s,t)^{\text{th}}$ element represents two times the kinship coefficient, which is the probability that two alleles, one randomly chosen from individual s in pedigree i and the other from individual t, are 'identical by descent', i.e. come from same common ancestor (Kohler et al., 2011). The second variance component accounts for shared environmental effect within each family, while the third term quantifies other sources of variation unique to an individual.

Following basic probability, the kinship coefficient of a parent-child pair is 1/4, a full sibling pair or non-identical (or dizygous = DZ) twins is 1/4, and for identical (or monozygous = MZ) twins is 1/2 in a nuclear pedigree. Following this, we can construct the $\mathbf{\Phi}_i$ matrices for different types of families:

$$\mathbf{\Phi}_{MZ} = \begin{bmatrix} 1 & 0 & 1/2 & 1/2 \\ 0 & 1 & 1/2 & 1/2 \\ 1/2 & 1/2 & 1 & 1 \\ 1/2 & 1/2 & 1 & 1 \end{bmatrix}, \mathbf{\Phi}_{DZ} = \begin{bmatrix} 1 & 0 & 1/2 & 1/2 \\ 0 & 1 & 1/2 & 1/2 \\ 1/2 & 1/2 & 1 & 1/2 \\ 1/2 & 1/2 & 1/2 & 1 \end{bmatrix}, \mathbf{\Phi}_{Adopted} = \mathbf{I}_4$$

for families with parents (indices 1 and 2) and MZ twins, DZ twins, or two adopted children (indices 3 and 4), respectively.

3 Variable selection using e-values

We present the details of our methodology in this section. Sections 3.1 and 3.2 summarize the existing method of e-values that performs best subset variable selection in a wide range

of statistical models (Majumdar and Chatterjee, 2017). We build on this framework in Section 3.3, where we present new results for better detection of weak SNP signals. Section 3.4 elaborates on the bootstrap implementation of this methodology using the model in (2.1).

3.1 Models and evaluation maps

In a general modelling situation where one needs to estimate a set of parameters $\theta \in \mathbb{R}^p$ from a triangular array of samples $\mathcal{B}_n = \{B_{n1}, \ldots, B_{nk_n}\}$ at stage n, any hypothesis or statistical model corresponds to a subset of the full parameter space. Here we consider the model spaces $\mathbf{\Theta}_{mn} \subseteq \mathbb{R}^p$ in which some elements of the parameter vector have fixed values, while others are estimated from the data. Formally, a generic parameter vector $\theta_{mn} \in \mathbf{\Theta}_{mn}$ consists of entries

$$\theta_{mnj} = \begin{cases} \text{Unknown } \theta_{mnj} & \text{for } j \in \mathcal{S}_n; \\ \text{Known } c_{nj} & \text{for } j \notin \mathcal{S}_n. \end{cases}$$

for some $\mathcal{S}_n \subseteq \{1, \ldots, p\}$. Thus the estimable index set $\mathcal{S}_n$ and fixed elements $c_n = (c_{nj} : j \notin \mathcal{S}_n)$ fully specify any model in this setup.

At this point, the original framework in Majumdar and Chatterjee (2017) introduces a few concepts to provide a detailed treatment considering a general scenario. For our specific problem, i.e. variable selection, we only require vastly simplified versions of them. We consider sample size $k_n = n$ for all n, and assume constant sequences of candidate models: $\mathcal{M}_n = \mathcal{M}$ for all n. We also drop the subscripts in $\mathcal{S}_n$ and c_n. Thus the 'full model', i.e. the model with all covariates is denoted by $\mathcal{M}_* = (\{1, \ldots, p\}, \emptyset)$.

Given data of size n, we obtain the full model estimates as minimizers of an estimating equation:

$$\hat{\theta} = \arg\min_{\theta} \Psi(\theta) = \arg\min_{\theta} \sum_{i=1}^{n} \Psi_i(\theta, B_i) \tag{3.1}$$

The only condition we impose on these generic estimating functionals $\Psi_i(.)$ are:
(P1) The population version of (3.1) has a unique minimizer θ_0, i.e.

$$\theta_0 = \arg\min_{\theta} \mathbb{E} \sum_{i=1}^{n} \Psi_i(\theta, B_i)$$

(P2) There exist a sequence of positive numbers $a_n \uparrow \infty$ and a p-dimensional probability distribution $\mathbb{T}_0$ such that $a_n(\hat{\theta} - \theta_0) \rightsquigarrow \mathbb{T}_0$.

We designate θ_0 as the *true parameter vector*, some elements of which are potentially set to 0. We can now classify any candidate model $\mathcal{M}$ into one of the two classes: the ones that satisfy $\theta_0 \in \mathbf{\Theta}_m$, and the ones that do not. We denote these two types of models by *adequate* and *inadequate models*, respectively. Given the data and unknown θ_0, we want to determine if a candidate model is adequate or inadequate.

For this we need coefficient estimates $\hat{\theta}_m$ corresponding to a model. We do so by just replacing elements of $\hat{\theta}$ not in $\mathcal{S}$ by corresponding elements of c. This means that for the j^{th} element, $j = 1, \ldots, p$, we have

$$\hat{\theta}_{mj} = \begin{cases} \text{Unknown } \hat{\theta}_j & \text{for } j \in \mathcal{S}; \\ \text{Known } c_j & \text{for } j \notin \mathcal{S} \end{cases}$$

We denote the probability distribution of a random variable $\mathbf{T}$ by $[\mathbf{T}]$. With this notation, we aim to compare the above model estimate distributions with the full model distribution, i.e. $[\hat{\theta}_m]$ with $[\hat{\theta}]$. For this we define an *evaluation map* function $E : \mathbb{R}^p \times \tilde{\mathbb{R}}^p \to [0, \infty)$ that measures the relative position of $\hat{\theta}_m$ with respect to $[\hat{\theta}]$. Here $\tilde{\mathbb{R}}^p$ is the set of probability measures on $\mathbb{R}^p$. We assume that E satisfies the following conditions:
(E1) For any probability distribution $\mathbb{G} \in \tilde{\mathbb{R}}^p$ and $x \in \mathbb{R}^p$, E is invariant under location and scale transformations:

$$E(x, \mathbb{G}) = E(ax + b, [a\mathbf{G} + b]); \quad a \in \mathbb{R} \neq 0, b \in \mathbb{R}^p$$

where the random variable $\mathbf{G}$ has distribution $\mathbb{G}$.
(E2) The evaluation map E is lipschitz continuous under the first argument:

$$|E(x, \mathbb{G}) - E(y, \mathbb{G})| < \|x - y\|^{\alpha}; \quad x, y \in \mathbb{R}^p, \alpha > 0$$

(E3) Suppose $\{\mathbb{Y}_n\}$ is a tight sequence of probability measures in $\tilde{\mathbb{R}}^p$ with weak limit $\mathbb{Y}_\infty$. Then $E(x, \mathbb{Y}_n)$ converges uniformly to $E(x, \mathbb{Y}_\infty)$.
(E4) Suppose $\mathbf{Z}_n$ is a sequence of random variables such that $\|\mathbf{Z}_n\| \xrightarrow{P} \infty$. Then $E(\mathbf{Z}_n, \mathbb{Y}_n) \xrightarrow{P} 0$.

For any $x \in \mathbb{R}^p$ and $[\mathbf{X}] \in \tilde{\mathbb{R}}^p$ with a positive definite covariance matrix $\mathbb{V}\mathbf{X}$, following are examples of the evaluations functions covered by the above set of conditions:

$$E_1(x, [\mathbf{X}]) = \left[1 + \left\| \frac{x - \mathbb{E}\mathbf{X}}{\sqrt{\text{diag}(\mathbb{V}\mathbf{X})}} \right\|^2\right]^{-1}; \quad E_2(x, [\mathbf{X}]) = \exp\left[-\left\| \frac{x - \mathbb{E}\mathbf{X}}{\sqrt{\text{diag}(\mathbb{V}\mathbf{X})}} \right\|\right] \tag{3.2}$$

Data depths (Tukey, 1975; Zuo and Serfling, 2000; Zuo, 2003) also constitute a broad class of point-to-distribution proximity functions that satisfy the above regularity conditions for evaluation maps. Indeed, Majumdar and Chatterjee (2017) used halfspace depth (Tukey, 1975) as evaluation function to perform model selection. However, the conditions (E1) and (E4) are weaker than those imposed on a traditional depth function (Zuo and Serfling, 2000). Conditions (E2) and (E3) are not required of depth functions in general, but they arise implicitly in several implementations of data depth (Mosler, 2013). The theoretical results we state here are based on a general evaluation map and not depth functions *per se*. To emphasize this point, in the numerical sections we use the non-depth evaluation functions E_1 and E_2 as in (3.2) above.

3.2 Model selection using e-values

Depending on the choice of the data sequence $\mathcal{B}_n$, $E(\hat{\theta}_m, [\hat{\theta}])$ can take different values. For any candidate model $\mathcal{M}$, we denote the distribution of the corresponding random evaluation map by $\mathbb{E}_{mn}$. For simplicity we drop the n in its subscript, i.e. $\mathbb{E}_{mn} \equiv \mathbb{E}_m$. These distributions are informative of how model estimates behave, and we use them as a tool to distinguish between inadequate and adequate models. Given a single set of samples, we use resampling schemes that satisfy standard regularity conditions (Majumdar and Chatterjee, 2017) to get consistent approximations of $\mathbb{E}_m$.

We now define a quantity called the **e-value** to compare the different model estimates and eventually perform selection of important SNPs from a multi-SNP model. Loosely construed, any functional of the evaluation map distribution $\mathbb{E}_m$ that can act as model evidence is an e-value. For example, Majumdar and Chatterjee (2017) took the mean functional of $\mathbb{E}_m$ (say $\mu(\mathbb{E}_m)$) as e-value, and proved a result that, when adapted to our setting, states as:

Theorem 3.1. *Consider estimators satisfying conditions (P1) and (P2), and an evaluation map E satisfying the conditions (E1), (E2) and (E4). Also suppose that*

$$\lim_{n\to\infty} \mu(\mathbb{Y}_n) = \mu(\mathbb{Y}_\infty) < \infty$$

for any tight sequence of probability measures $\{\mathbb{Y}_n\}$ in $\tilde{\mathbb{R}}^p$ with weak limit $\mathbb{Y}_\infty$. Then as $n \to \infty$,

1. *For the full model, $\mu(\mathbb{E}_*) \to \mu_\infty$ for some $0 < \mu_\infty < \infty$;*
2. *For any adequate model, $|\mu(\mathbb{E}_m) - \mu(\mathbb{E}_*)| \to 0$;*
3. *For any inadequate model, $\mu(\mathbb{E}_m) \to 0$.*

Taking data depths as evaluation functions leads to a further result that $\mu(\mathbb{E}_*) < \mu(\mathbb{E}_m)$ for any adequate model $\mathcal{M}$ and large enough n. Following this, non-zero indices of θ_0 (say $\mathcal{S}_0$) can be recovered through a fast algorithm that has these generic steps:

1. Estimate the e-value of the full model, i.e. $\hat{\mu}(\mathbb{E}_*)$, through bootstrap approximation of $\mathbb{E}_*$;
2. For the j^{th} predictor, $j = 1, \ldots, p$, consider the model with the j^{th} coefficient of $\hat{\theta}$ replaced by 0, and get its e-value. Suppose this is $\hat{\mu}(\mathbb{E}_{-j})$;
3. Collect the predictors for which $\hat{\mu}(\mathbb{E}_{-j}) < \hat{\mu}(\mathbb{E}_*)$. Name this index set $\hat{\mathcal{S}}_0$: this is the estimated set of non-zero coefficients in $\hat{\theta}$.

As $n \to \infty$, the above algorithm provides consistent model selection, i.e. $\mathbb{P}(\hat{\mathcal{S}}_0 = \mathcal{S}_0) \to 1$, with the underlying resampling distribution having mean 1 and variance τ_n^2 such that $\tau_n \to \infty, \tau_n/\sqrt{n} \to 0$ as $n \to \infty$ (Majumdar and Chatterjee, 2017).

3.3 Quantiles of $\mathbb{E}_m$ as e-values

When true signals are weak, the above method of variable selection leads to very conservative estimates of non-zero coefficient indices, i.e. a large number of false positives in a sample setting. This happens because even though at the population level $\mu(\mathbb{E}_*)$ separates the population means of inadequate model sampling distributions and those of adequate models, for weak signals bootstrap estimates of adequate model distributions almost overlap with those of the full model.

Figure 3.1 demonstrates this phenomenon in our simulation setup. Here we analyze data on 250 families with monozygotic twins, each individual being genotyped for 50 SNPs. Four of these 50 SNPs are causal: each having a heritability of $h/6\%$ with respect to the total error variation present. The four panels show density plots of $\hat{\mathbb{E}}_{-j}$ for $j = 1, \ldots, p$, as well as $\hat{\mathbb{E}}_*$: based on resampling schemes with four different values of the standard deviation parameter $s \equiv s_n = \tau_n/\sqrt{n}$. While smaller values of s are able to separate out the bootstrap estimates of $\mathbb{E}_{-j}$ for inadequate and adequate models, all the density plots are to the left of the curve corresponding to the full model.

However, notice that the inadequate and adequate model distributions have different tail behaviors for smaller values of s, and setting an appropriate upper threshold to tail probabilities for a suitable fixed quantile of these distributions with respect to the full model distribution can possibly provide a better separation of the two types of distributions. For this reason we use tail quantiles as e-values.

We denote the q^{th} population quantile of $\mathbb{E}_m$ by $c_q(\mathbb{E}_m)$. Then we have equivalent results to Theorem 3.1 as $n \to \infty$:

Theorem 3.2. *Given that the estimator $\hat{\theta}$ satisfies conditions (P1) and (P2), and the evaluation map satisfies conditions (E1)-(E4), we have*

$$c_q(\mathbb{E}_*) \to c_{q,\infty} < \infty \tag{3.3}$$

$$|c_q(\mathbb{E}_m) - c_q(\mathbb{E}_*)| \to 0 \text{ when } \mathcal{M} \text{ is adequate} \tag{3.4}$$

$$c_q(\mathbb{E}_m) \to 0 \text{ when } \mathcal{M} \text{ is inadequate} \tag{3.5}$$

When the q^{th} quantile is taken as the e-value instead of the mean, we set a lower detection threshold than the same functional on the full model, i.e. choose all j such that $c_q(\mathbb{E}_{-j}) < c_{qt}(\mathbb{E}_*), 0 < t < 1$ to be included in the model. The choice of t potentially depends on several factors such as the value of quantile evaluated, the statistical model used, sample size and degree of sparsity of parameters in the data generating process. We illustrate this point on simulated data in Section 4.

3.4 Bootstrap procedure

We use generalized bootstrap (Chatterjee and Bose, 2005) to obtain approximations of the sampling distributions $\mathbb{E}_{-j}$ and $\mathbb{E}_*$. It calculates bootstrap equivalents of the parameter

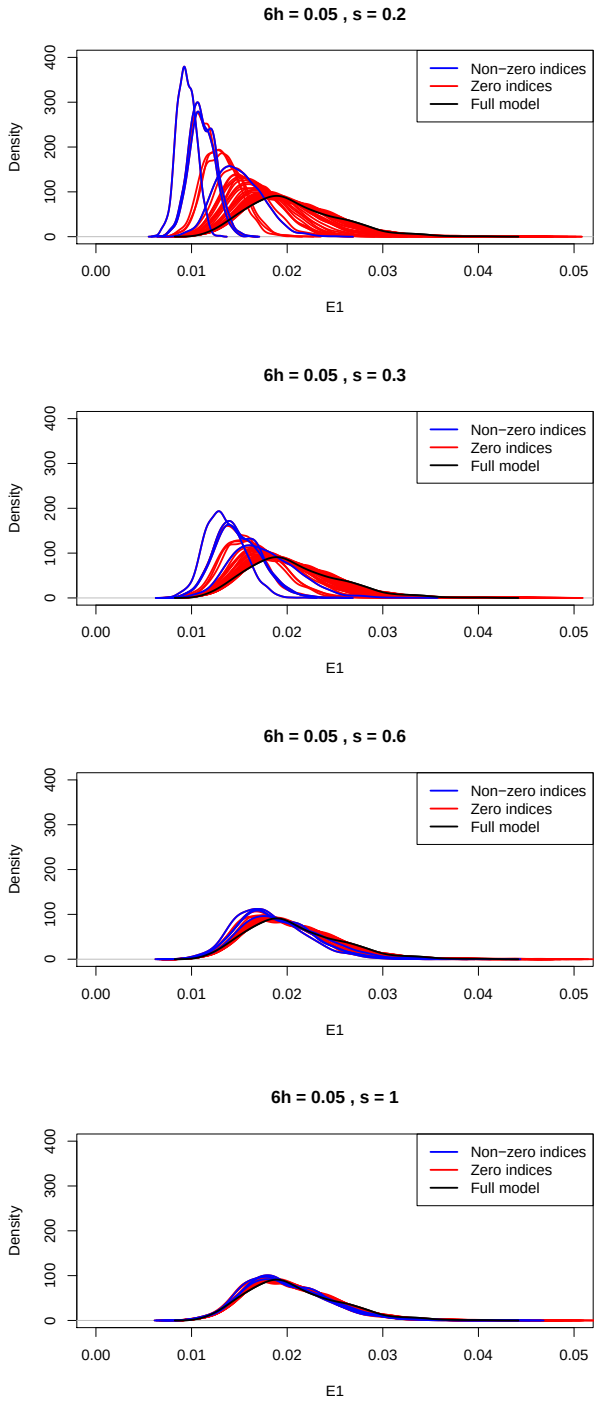

Figure 3.1: Density plots of bootstrap approximations for $\mathbb{E}_*$ and $\mathbb{E}_{-j}$ for all j in simulation setup, with $s = 0.2, 0.3, 0.6, 1$

estimate $\hat{\theta}$ by minimizing a version of the estimating equation in (3.1) with random weights:

$$\hat{\theta}_w = \arg\min_{\theta} \sum_{i=1}^{n} \mathbb{W}_i \Psi_i(\theta, B_i) \tag{3.6}$$

The resampling weights $(\mathbb{W}_1, \ldots, \mathbb{W}_n)$ are non-negative exchangeable random variables chosen independent of the data, and satisfy the following conditions:

$$\mathbb{E}\mathbb{W}_1 = 1; \quad \mathbb{V}\mathbb{W}_1 = \tau_n^2 \uparrow \infty; \quad \tau_n^2 = o(a_n^2) \tag{3.7}$$

$$\mathbb{E}W_1 W_2 = O(n^{-1}); \quad \mathbb{E}W_1^2 W_2^2 \to 1; \quad \mathbb{E}W_1^4 < \infty \tag{3.8}$$

with $W_i := (\mathbb{W}_i - 1)/\tau_n; i = 1, \ldots, n$ being the centered and scaled resampling weights. Under standard regularity conditions on the estimating functional $\Psi(.)$ (Chatterjee and Bose, 2005; Majumdar and Chatterjee, 2017) and conditional on the data, $(a_n/\tau_n)(\hat{\theta}_w - \hat{\theta})$ converges to the same asymptotic distribution as $a_n(\hat{\theta} - \theta_0)$, i.e. $\mathbb{T}_0$.

We use empirical quantiles of the full model bootstrap samples as the quantile e-value estimates. Specifically, we go through the following steps:

1. Fix $q, t \in (0, 1)$;
2. Generate two independent set of bootstrap weights, of size R and R_1, and obtain the corresponding approximations to the full model sampling distribution, say $[\hat{\theta}_r]$ and $[\hat{\theta}_{r_1}]$;
3. For $j = 1, 2, \ldots p$ and estimate the e-value of the j^{th} predictor as the empirical q^{th} quantile of $\hat{\mathbb{E}}_{-j} := [E(\hat{\theta}_{r,-j}, [\hat{\theta}_{r_1}])]$, with $\hat{\theta}_{r,-j}$ obtained from $\hat{\theta}_r$ by replacing the j^{th} coordinate with 0;
4. Estimate the set of non-zero covariates as

$$\hat{\mathcal{S}}_0 = \{j : c_q(\hat{\mathbb{E}}_{-j}) < c_{qt}(\hat{\mathbb{E}}_*)\};$$

Conditions (3.7) and (3.8) on the resampling weights ensure bootstrap-consistent approximation of the evaluation map quantiles:

Theorem 3.3. *Given the estimator $\hat{\theta}$ and evaluation map E in Theorem 3.2, and a generalized bootstrap scheme satisfying (3.7) and (3.8), we get*

$$|c_q(\hat{\mathbb{E}}_m) - c_q(\hat{\mathbb{E}}_*)| \xrightarrow{P_n} o_P(1) \text{ when } \mathcal{M} \text{ is adequate} \tag{3.9}$$

$$c_q(\hat{\mathbb{E}}_m) \xrightarrow{P_n} o_P(1) \text{ when } \mathcal{M} \text{ is inadequate} \tag{3.10}$$

where P_n is probability conditional on the data.

Generalized bootstrap covers a large array of resampling procedures, for example the m-out-of-n bootstrap and a scale-enhanced version of the bayesian bootstrap. Furthermore, given that $\Psi_i(.)$ are twice differentiable in a neighborhood of θ_0 and some other conditions in Chatterjee and Bose (2005), there is an approximate representation of $\hat{\theta}_w$:

$$\hat{\theta}_w = \hat{\theta} - \frac{\tau_n}{a_n}\left[\sum_{i=1}^{n} W_i \Psi_i''(\hat{\theta}, B_i)\right]^{-1} \sum_{i=1}^{n} W_i \Psi_i'(\hat{\theta}, B_i) + \mathbf{R}_{wn} \tag{3.11}$$

with $\mathbb{E}_w \|\mathbf{R}_{wn}\|^2 = o_P(1)$.

Given the full model estimate $\hat{\theta}$, and the score vectors $\Psi_i'(\hat{\theta}, B_i)$ and hessian matrices $\Psi_i''(\hat{\theta}, B_i)$, (3.11) allows us to obtain multiple copies of $\hat{\theta}_w$ through Monte-Carlo simulation of several arrays of bootstrap weights. This bypasses the need to fit the full model for each bootstrap sample, resulting in extremely fast computation of e-values.

We adapt the approximation of (3.11) to the LMM in (2.1). We first obtain the maximum likelihood estimates $\hat{\beta}_g, \hat{\sigma}_a^2, \hat{\sigma}_c^2, \hat{\sigma}_e^2$ through fitting the LMM. Then we replace the variance components in (2.2) with corresponding estimates to get $\hat{\mathbf{V}}_i$ for i^{th} pedigree, and aggregate them to get the covariance matrix estimate for all samples:

$$\hat{\mathbf{V}} = \text{diag}(\hat{\mathbf{V}}_1, \ldots, \hat{\mathbf{V}}_m)$$

We take m random draws from Gamma$(1,1) - 1$, say $\{w_{r1}, \ldots, w_{rm}\}$, as resampling weights in (3.11), using the same weight for all members of a pedigree. Consequently, the bootstrapped coefficient estimate $\hat{\beta}_{rg}$ has the following representation:

$$\hat{\beta}_{rg} \simeq \hat{\beta}_g + \frac{\tau_n}{\sqrt{n}}(\mathbf{G}^T\hat{\mathbf{V}}^{-1}\mathbf{G})^{-1}\mathbf{W}_r\mathbf{G}^T\hat{\mathbf{V}}^{-1}(y - \mathbf{G}\hat{\beta}_g) \tag{3.12}$$

with $\mathbf{G} = (\mathbf{G}_1^T, \ldots, \mathbf{G}_m^T)^T$ and $\mathbf{W}_r = \text{diag}(w_{r1}\mathbf{I}_4, \ldots, w_{rm}\mathbf{I}_4)$. Finally we repeat the procedure for two independent sets of resampling weights, say of sizes R and R_1, to obtain two collections of bootstrapped estimates $\{\hat{\beta}_{1g}, \ldots, \hat{\beta}_{Rg}\}$.

4 Simulation

We now evaluate the performance of the above formulation of quantile e-values in a simulation setup. For this, consider the model in (2.1) with no environmental covariates. We consider familes with MZ twins and first generate the SNP matrices $\mathbf{G}_i$. We take a total of $p_g = 50$ SNPs, and generate them in correlated blocks of 6, 4 ,6, 4 and 30 to simulate correlation among SNPs in the genome. We set the correlation between two SNPs inside a block at 0.7, and consider the blocks to be uncorrelated. For each parent we generate two independent vectors of length 50 with the above correlation structure, and entries within each block being 0 or 1 following Bernoulli distributions with probabilities 0.2, 0.4, 0.4, 0.25 and 0.25 (Minor Allele Frequency or MAF) for SNPs in the 5 blocks, respectively. The genotype of a person is then determined by taking the sum of these

two vectors: thus entries in $\mathbf{G}_i$ can take the values 0, 1 or 2. Finally we set the common genotype of the twins by randomly choosing one allele vector from each of the parents and taking their sum.

We repeat the above process for $m = 250$ families. In GWAS generally each associated SNP explains only a small proportion of the overall variability of the trait. To reflect this in our simulation setup, we assume that the first entries in each of the first four blocks above are causal, and each of them explains $h/(\sigma_a^2 + \sigma_c^2 + \sigma_e^2)\%$ of the overall variability. The term h is known as the *heritability* of the corresponding SNP. The value of the non-zero coefficient in k-th block: $k = 1, ..., 4$, say β_k is calculated using the formula:

$$\beta_k = \sqrt{\frac{h}{100(\sigma_a^2 + \sigma_c^2 + \sigma_e^2).2\text{MAF}_k(1 - \text{MAF}_k)}} \tag{4.1}$$

We fix the following values for the error variance components: $\sigma_a^2 = 4, \sigma_c^2 = 1, \sigma_e^2 = 1$, and generate pedigree-wise response vectors $y_1, \ldots, y_{250}$ using the above setup. To consider different SNP effect sizes, we repeat the above setup for $h \in \{10, 7, 5, 3, 2, 1, 0\}$, generating 1000 datasets for each value of h.

4.1 Methods and metrics

For this simulated data, we compare our e-value based approach using the evaluation maps E_1 and E_2 in (3.2) with two other methods:

(1) Model selection on linear model: Here we ignore the dependency structure within families by training linear models on the simulated data and selecting SNPs with non-zero effects by backward deletion using a modification of the BIC called mBIC2. This has been showed to give better results than single-SNP analysis in a GWAS with unrelated individuals (Frommelet et al., 2012) and provides approximate False Discovery Rate (FDR) control at level 0.05 (Bogdan et al., 2011).

(2) Single-marker mixed model: We train single-SNP versions of (2.1) using a fast approximation of the Generalized Least Squares procedure (named Rapid Feasible Generalized Least Squares or RFGLS: Li et al. (2011)), obtain marginal p-values from corresponding t-tests and use the Benjamini-Hochberg (BH) procedure to select significant SNPs at FDR = 0.05.

With the e-value being the q^{th} quantile of the evaluation map distribution, we set the detection threshold value at the t^{th} multiple of q for some $0 < t < 1$. This means all indices j such that the q^{th} quantile of the bootstrap approximation of $\mathbb{E}_{-j}$ is less than the tq^{th} quantile of the bootstrap approximation of $\mathbb{E}_*$ get selected as the set of active predictors. To enforce stricter control on the selected set of SNPs we repeat this for $q \in \{0.5, 0.6, 0.7, 0.8, 0.9\}$, and take the SNPs that get selected for *all* values of q as the final set of selected SNPs.

Since the above procedure depends on the bootstrap standard deviation parameter s, we repeat the process for $s \in \{0.3, 0.15, \ldots, 0.95, 2\}$, and take as the final estimated set of SNPs the SNP set $\hat{\mathcal{S}}_t(s)$ that minimizes fixed effect prediction error (PE) on an

independently generated test dataset $\{(y_{test,i}, \mathbf{G}_{test,i}), i = 1, \ldots, 250\}$ from the same setup above:

$$\mathrm{PE}_t(s) = \sum_{i=1}^{250} \sum_{j=1}^{4} \left(y_{test,ij} - g_{test,ij}^T \hat{\beta}_{\hat{\mathcal{S}}_t(s)} \right)^2;$$
$$\hat{\mathcal{S}}_t = \arg\min_s \mathrm{PE}_t(s)$$

We use the following metrics to evaluate each method we implement: (1) True Positive (TP), which is the proportion of causal SNPs detected; (2) True Negative (TN), which is the proportion of non-causal SNPs undetected; (3) Relaxed True Positive (RTP), which is the: proportion of detecting any SNP in each of the 4 blocks with causal SNPs, i.e. for the selected index set by some method m, say $\hat{\mathcal{S}}_m$,

$$\mathrm{RTP}(\hat{\mathcal{S}}_m) = \frac{1}{4} \sum_{i=1}^{4} \mathbb{I}(\text{Block } i \cap \hat{\mathcal{S}}_m \neq \emptyset)$$

and finally (4) Relaxed True Negative (RTN), which is the proportion of SNPs in block 5 undetected. We consider the third and fourth metrics to cover situations in which the causal SNP is not detected itself, but highly correlated SNPs with the causal SNP are. This is common in GWAS (Frommelet et al., 2012). Finally, we average all the above proportions over 1000 replications, and repeat the process for two different ranges of t for E_1 and E_2.

4.2 Results

We present the simulation results in table 4.1. For all heritability values, applying mBIC2 on linear models performs poorly compared to applying RFGLS and then correcting for multiple testing. This is expected because the linear model ignores within-family error components.

Our method works better than the two competing methods for detecting true signals across different values of h: the average TP rate going down slowly than other methods across the majority of choices for t. Both mBIC2 and RFGLS+BH have very high true negative detection rates, which is matched by our method for higher values of q. Since all reduced model distributions reside on the left of the full model distribution, we expect the variable selection process to turn more conservative at lower values of t.This effect is more noticeable for lower q, indicating that the right tails of evaluation map distributions are more useful for this purpose. Finally for $h = 0$, we report only TN and RTN values since no signals should ideally be detected: in terms of this a value of $q = 0.9$ or $q = 0.5$ leads to the same TN and RTN performance as RFGLS+BH for all choices of t.

RTP performances for all methods are better than the corresponding TP/TN performances. However, for mBIC2 this seems to be due to detecting SNPs in the first four blocks by chance since for $h = 0$ its RTN is less than TN. Also E_2 seems to perform slightly better than E_1, in the sense that it yields a higher TP (or RTP) while having the same TN (or RTN) rates.

Method		$h = 10$	$h = 7$	$h = 5$	$h = 3$	$h = 2$	$h = 1$	$h = 0$
mBIC2		0.79/0.99	0.59/0.99	0.41/0.99	0.2/0.99	0.11/0.99	0.05/0.99	-/0.99
RFGLS+BH		0.95/0.92	0.82/0.95	0.62/0.97	0.29/0.98	0.14/0.99	0.04/1	-/1
E_1	$t = \exp(-1)$	0.95/0.98	0.87/0.97	0.74/0.97	0.47/0.97	0.28/0.97	0.12/0.98	-/0.99
	$t = \exp(-2)$	0.94/0.98	0.85/0.98	0.69/0.98	0.43/0.98	0.25/0.98	0.09/0.99	-/0.99
	$t = \exp(-3)$	0.94/0.99	0.82/0.98	0.65/0.98	0.37/0.99	0.2/0.99	0.07/0.99	-/1
	$t = \exp(-4)$	0.92/0.99	0.79/0.99	0.61/0.99	0.32/0.99	0.17/0.99	0.06/1	-/1
	$t = \exp(-5)$	0.9/0.99	0.75/0.99	0.55/0.99	0.26/1	0.13/1	0.04/1	-/1
E_2	$t = 0.8$	0.97/0.98	0.9/0.97	0.79/0.96	0.54/0.96	0.34/0.97	0.15/0.98	-/0.99
	$t = 0.74$	0.96/0.98	0.88/0.97	0.75/0.97	0.48/0.97	0.29/0.98	0.12/0.98	-/0.99
	$t = 0.68$	0.95/0.99	0.87/0.98	0.72/0.98	0.45/0.98	0.26/0.98	0.1/0.99	-/0.99
	$t = 0.62$	0.95/0.99	0.84/0.98	0.68/0.98	0.4/0.99	0.22/0.99	0.09/0.99	-/0.99
	$t = 0.56$	0.94/0.99	0.82/0.99	0.65/0.99	0.36/0.99	0.19/0.99	0.07/1	-/1
	$t = 0.5$	0.92/0.99	0.79/0.99	0.6/0.99	0.31/0.99	0.16/1	0.05/1	-/1

Method		$h = 10$	$h = 7$	$h = 5$	$h = 3$	$h = 2$	$h = 1$	$h = 0$
mBIC2		0.84/0.99	0.66/0.99	0.48/0.99	0.26/0.99	0.16/0.99	0.08/0.99	-/0.98
RFGLS+BH		0.96/0.99	0.83/0.99	0.64/0.99	0.32/0.99	0.16/1	0.05/1	-/1
E_1	$t = \exp(-1)$	0.95/0.98	0.87/0.97	0.75/0.97	0.5/0.97	0.32/0.98	0.15/0.98	-/0.98
	$t = \exp(-2)$	0.94/0.99	0.85/0.98	0.71/0.98	0.45/0.98	0.28/0.98	0.12/0.99	-/0.98
	$t = \exp(-3)$	0.94/0.99	0.83/0.99	0.67/0.99	0.39/0.99	0.22/0.99	0.09/0.99	-/0.99
	$t = \exp(-4)$	0.92/0.99	0.8/0.99	0.62/0.99	0.33/0.99	0.18/0.99	0.07/1	-/1
	$t = \exp(-5)$	0.9/0.99	0.75/0.99	0.56/0.99	0.27/1	0.14/1	0.05/1	-/1
E_2	$t = 0.8$	0.97/0.98	0.91/0.97	0.8/0.96	0.57/0.96	0.38/0.97	0.2/0.98	-/0.97
	$t = 0.74$	0.96/0.98	0.89/0.98	0.76/0.97	0.51/0.97	0.33/0.98	0.15/0.98	-/0.98
	$t = 0.68$	0.95/0.99	0.87/0.98	0.73/0.98	0.48/0.98	0.29/0.98	0.12/0.99	-/0.98
	$t = 0.62$	0.95/0.99	0.85/0.99	0.69/0.98	0.42/0.99	0.24/0.99	0.11/0.99	-/0.99
	$t = 0.56$	0.94/0.99	0.83/0.99	0.66/0.99	0.38/0.99	0.2/0.99	0.08/0.99	-/0.99
	$t = 0.5$	0.92/0.99	0.79/0.99	0.61/0.99	0.32/0.99	0.17/1	0.06/1	-/1

Table 4.1: (Top) Average True Positive (TP)/ True Negative (TN) rates for mBIC2, RFGLS+BH and the e-values method with E_1 and E_2 as evaluation maps and different values of t over 1000 replications, and (Bottom) Average Relaxed True Positive (RTP) and Relaxed True Negative (RTN) rates

Gene	Total no. of SNPs	No. of SNPs detected by		
		e-value	RFGLS+BH	mBIC2
GABRA2	11	5	0	0
ADH	44	3	1	0
OPRM1	47	25	1	0
CYP2E1	9	5	0	0
ALDH2	6	5	0	1
COMT	15	14	0	0
SLC6A3	18	4	0	0
SLC6A4	5	0	0	0
DRD2	17	0	0	1

Table 5.1: Table of analyzed genes and number of detected SNPs in them by the three methods

5 Analysis of the MCTFR data

We now apply the above methods on SNPs from the MCTFR dataset. We assume a nuclear pedigree structure, and for simplicity only analyze pedigrees with MZ and DZ twins. After setting aside samples with missing response variables, we end up with 1019 such 4-member families. We look at the effect of genetic factors behind the response variable pertaining to the amount of alcohol consumption, which is highly heritable in this dataset according to previous studies (McGue et al., 2013). We analyze SNPs inside some of the most-studied genes with respect to alcohol abuse: GABRA2, ADH1A, ADH1B, ADH1C, ADH4-ADH7, SLC6A3, SLC6A4, OPRM1, CYP2E1, DRD2, ALDH2, and COMT (Coombes, 2016) through separate gene-level models. Any of the ADH genes did not contain many SNPs individually, so we consider the SNPs in all seven of them together. We include sex, birth year, age and generation (parent or offspring) of individuals as covariates to control for their potential effect.

For model selection we use E_2 as the evaluation function because of its slighty better performance in the simulations. For each gene-level model, We train the LMM in (2.1) on 75% of randomly selected families, perform our e-values procedure for $s = 0.2, 0.4, \ldots, 2.8, 3, t = 0.1, 0.15, \ldots, 0.75, 0.8$; and select the set of SNPs that minimizes fixed effect prediction error on the data from the other 25% of families over this grid of (s, t).

As seen in Table 5.1, our e-value based technique detects a much higher number of SNPs than the two competing methods. Our method selects all but one SNP in the genes ALDH2 and COMT. These are small genes of size 50kb and 30kb, respectively, thus SNPs within them have more chance of being in high Linkage Disequilibrium (LD). On the other hand, it does not select any SNPs in SLC6A4 and DRD2. Variants of these genes are known to interact with each other and are jointly associated with multiple behavioral disorders (Karpyak et al., 2010; Wang et al., 2014).

Gene	Detected SNPs with known associations	Reference for associated SNP
GABRA2	rs1808851, rs279856: close to rs279858	Cui et al. (2012)
ADH genes	rs17027523: 20kb upstream of rs1229984	Multiple studies (https://www.snpedia.com/index.php/Rs1229984)
OPRM1	rs12662873: 1 kb upstream of rs1799971	Multiple studies (https://www.snpedia.com/index.php/Rs1799971)
CYP2E1	rs9419624: 600b downstream of rs4646976; rs9419702: 10kb upstream of rs4838767	Lind et al. (2012)
ALDH2	rs16941437: 10kb upstream of rs671	Multiple studies (https://www.snpedia.com/index.php/Rs671)
COMT	rs4680, rs165774	Voisey et al. (2011)
SLC6A3	rs464049	Huang et al. (2017)

Table 5.2: Table of detected SNPs with known references

A number of SNPs we detect (or SNPs situated close to them) have known associations with alcohol-related behavioral disorders. We summarize this in Table 5.2. Prominent among them are rs1808851 and rs279856 in the GABRA2 gene, which are at perfect LD with rs279858 in the larger, 7188-individual version of our twin studies dataset (Irons, 2012). This SNP is the marker in GABRA2 that is most frequently associated in the literature with alcohol abuse (Cui et al., 2012), but was not genotyped in our sample. A single SNP RFGLS analysis of the same twin studies data that used Bonferroni correction on marginal p-values missed the SNPs we detect (Irons, 2012): highlighting the advantage of our approach. We give a gene-wise discussion of associated SNPs, as well as information on all SNPs, in the supplementary material.

We plot the 90^{th} quantile e-value estimates in Figures 5.1, 5.2 and 5.3. We obtained gene locations, as well as the locations of coding regions of genes, i.e. exons, inside 6 of these 9 genes from annotation data extracted from the UCSC Genome Browser database (Rosenbloom et al., 2015). Exon locations were not available for OPRM1, CYP2E1 and DRD2. In general, SNPs tend to get selected in groups with neighboring SNPs, which suggests high LD. Also most of the selected SNPs either overlap or in close proximity to the exons, which underline their functional relevance.

6 Discussion and conclusion

To expand the above approach to a genome-wide scale, we need to incorporate strategies for dealing with the hierarchical structure of pathways and genes: there are only a few genes associated with a quantitative phenotype, which can be further attributed to a small proportion of SNPs inside each gene. To apply the e-values method here, it is plausible to start with an initial screening step to eliminate evidently non-relevant genes. Methods like the grouped Sure Independent Screening (Li et al., 2012) and min-P test (Westfall and Young, 1993) can be useful here. Following this, in a multi-gene predictor set, there are several possible strategies to select important genes *and* important SNPs in them. Firstly, one can use a two-stage e-value based procedure. The first stage is same as the method described in this paper, i.e. selecting important SNPs from each gene using multi-SNP models trained on SNPs in that gene. In the second stage, a model will be trained using the aggregated set of SNPs obtained in the first step, and a group selection procedure will be run on this model using e-values. This means dropping *groups* of predictors (instead of single predictors) from the full model, checking the reduced model e-values, and selecting a SNP group only if dropping it causes the e-value to go below a certain cutoff. Secondly, one can start by selecting important genes using an aggregation method of SNP-trait associations (e.g. Lamparter et al. (2016)) and then run the e-value based SNP selection on the set of SNPs within these genes. Thirdly, one can also take the aggregated set of SNPs obtained from running the e-values procedure on gene-level models, then use a fast screening method (e.g. RFGLS) to select a subset of those SNPs.

We plan to study merits and demerits of these strategies and the computational issues

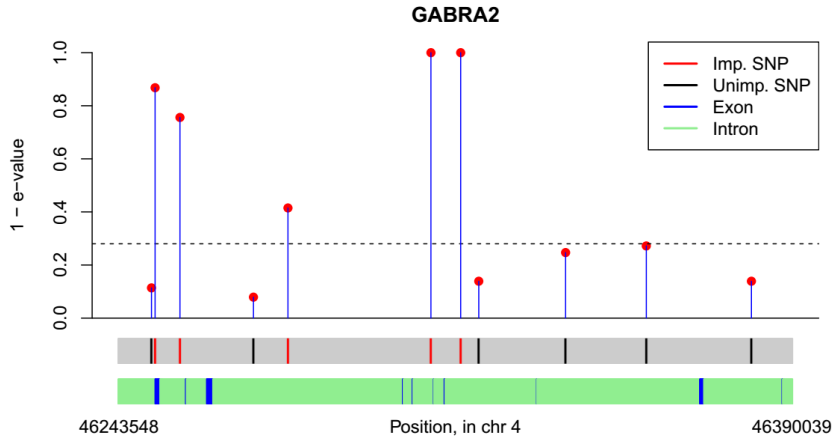

(a)

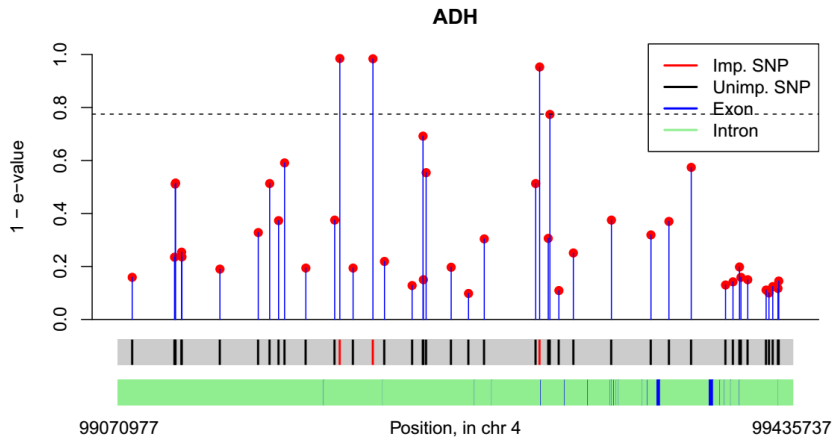

(b)

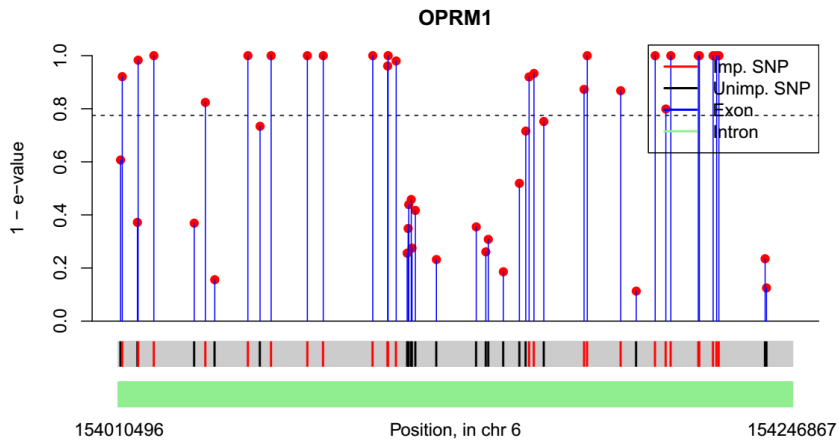

(c)

Figure 5.1: Plot of e-values for genes analyzed: (a) GABRA2, (b) ADH1 to ADH7, (c) OPRM1. For ease of visualization, $1 - e$-values are plotted in the y-axis.

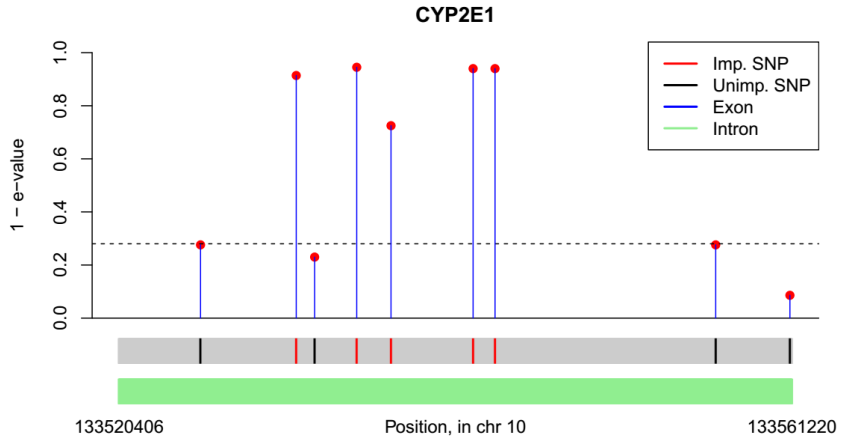

(d)

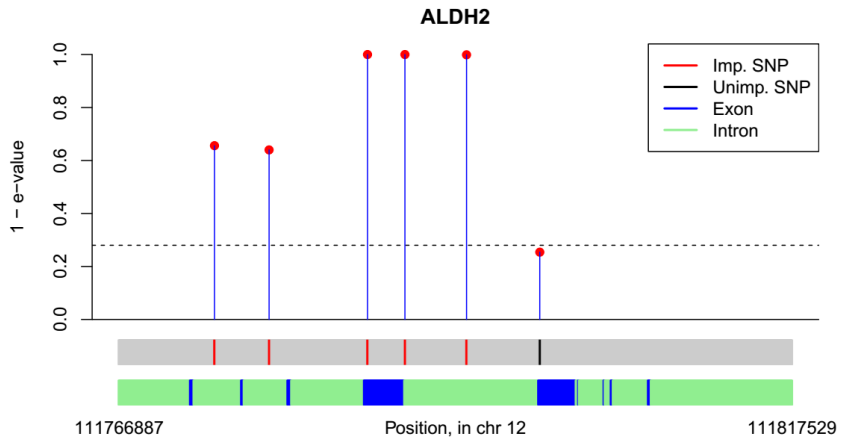

(e)

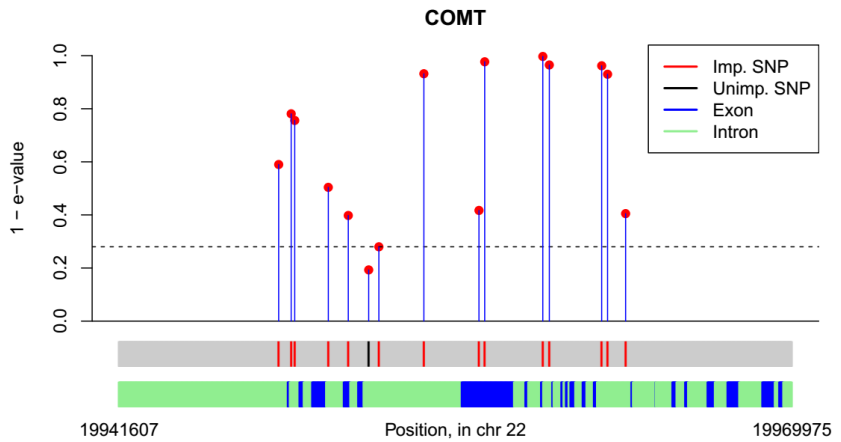

(f)

Figure 5.2: Plot of *e*-values for genes analyzed: (d) CYP2E1, (e) ALDH2, (f) COMT

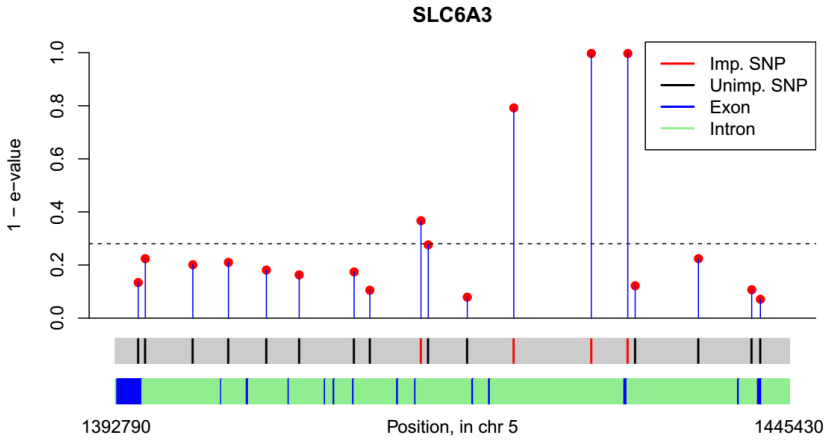

(g)

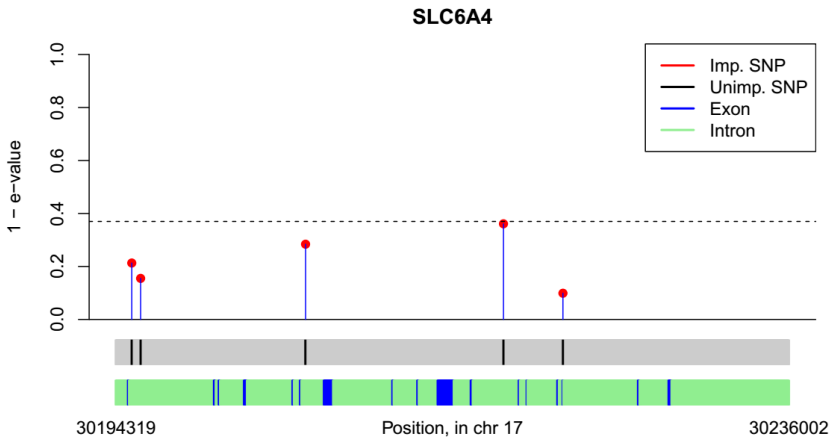

(h)

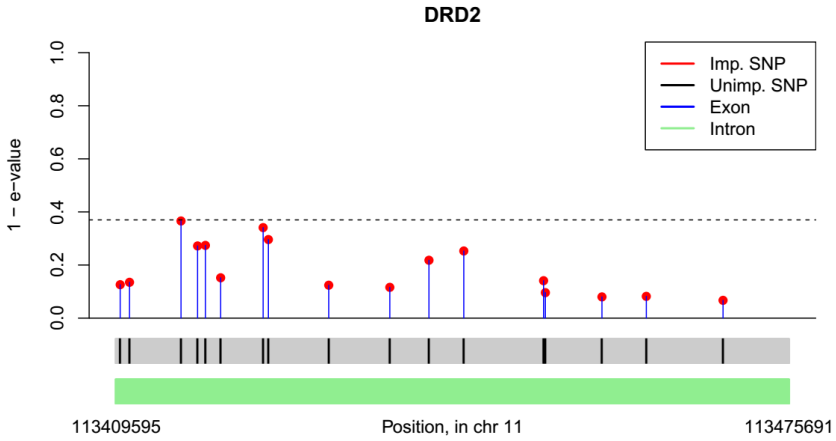

(i)

Figure 5.3: Plot of *e*-values for genes analyzed: (g) SLC6A3, (h) SLC6A4, (i) DRD2

associated with them in detail through synthetic studies as well as in the GWAS data from MCTFR. Finally, the current evaluation map based formulation requires the existence of an asymptotic distribution for the full model estimate. We plan to explore alternative formulation of evaluation maps under weaker conditions to bypass this, thus being able to tackle high-dimensional ($n < p$) situations.

References

Aulchenko, Y. S., Koning, D. J. D., and Haley, C. (2007). Genome-wide rapid association using mixed model and regression: a fast and simple method for genome-wide pedigree-based quantitative trait loci association analysis. *Nat. Genet.*, 177:577–585.

Benyamin, B., Visscher, P. M., and McRae, A. F. (2009). Family-based genome-wide association studies. *Pharmacogenomics*, 10(2):181–190.

Bogdan, M., Chakrabarti, A., Frommelet, F., and Ghosh, J. K. (2011). Asymptotic Bayes-optimality under sparsity of some multiple testing procedures. *Ann. Statist.*, 39:1551–1579.

Chang, C. Q., Yesupriya, A., Lowell, J. L., Pimentel, C. B., et al. (2014). A systematic review of cancer GWAS and candidate gene meta-analyses reveals limited overlap but similar effect sizes. *Eur, J. Hum. Genet.*, 22:402–408.

Chatterjee, S. and Bose, A. (2005). Generalized bootstrap for estimating equations. *Ann. Statist.*, 33:414–436.

Chen, H., Meigs, J. B., and Dupuis, J. (2013). Sequence Kernel Association Test for Quantitative Traits in Family Samples. *Genet. Epidemiol.*, 37:196–204.

Chen, W. M. and Abecasis, G. (2007). Family-based association tests for genome-wide association scans. *Am. J. Hum. Genet.*, 81:913–926.

Coombes, B., Basu, S., and McGue, M. (2017). A combination test for detection of gene-environment interaction in cohort studies. *Genet. Epidemiol.*, 41:396–412.

Coombes, B. J. (2016). *Tests for detection of rare variants and gene-environment interaction in cohort and twin family studies*. PhD thesis, University of Minnesota.

Cui, W. Y., Seneviratne, C., Gu, J., and Li, M. D. (2012). Genetics of GABAergic signaling in nicotine and alcohol dependence. *Hum. Genet.*, 131:843–855.

De Neve, J.-E., Mikhaylov, S., Dawes, C. T., et al. (2013). Born to Lead? A Twin Design and Genetic Association Study of Leadership Role Occupancy. *Leadersh Q*, 24:45–60.

Erblich, J. A., Lerman, C., Self, D. W., et al. (2005). Effects of dopamine d2 receptor (drd2) and transporter (slc6a3) polymorphisms on smoking cue-induced cigarette craving among african-american smokers. *Mol. Psychiatry*, 10:407–414.

Frommelet, F., Ruhaltinger, F., Twaróg, P., and Bogdan, M. (2012). Modified versions of Bayesian Information Criterion for genome-wide association studies. *Comput. Stat. Data Anal.*, 56:1038–1051.

Gelernter, J., Kranzler, H. R., Sherva, R., Almasy, L., et al. (2014). Genome-wide association study of alcohol dependence: significant findings in African- and European-Americans including novel risk loci. *Mol. Psychiatry*, 19:41–49.

Hicks, B. M., Schalet, B. D., Malone, S., Iacono, W. G., and McGue, M. (2011). Psychometric and Genetic Architecture of Substance Use Disorder and Behavioral Disinhibition Measures for Gene Association Studies. *Behav Genet.*, 41:459–475.

Huang, C.-C., Kuo, S.-C., Weh, Y.-W., et al. (2017). The SLC6A3 gene possibly affects susceptibility to late-onset alcohol dependence but not specific personality traits in a Han Chinese population. *PLoS ONE*, 12(2):e0171170.

Iacono, W. G., Carlson, S. R., Taylor, J., Elkins, I. J., and McGue, M. (1999). Behavioral disinhibition and the development of substance use disorders: Findings from the Minnesota Twin Family Study. *Dev. Psychopathol.*, 11:869–900.

Ionita-Laza, I., Lee, S., Makarov, V., Buxbaum, J. D., and Lin, X. (2013). Family-based association tests for sequence data, and comparisons with population-based association tests. *Eur. J. Hum. Genet.*, 21:1158–1162.

Irons, D. E. (2012). *Characterizing specific genetic and environmental influences on alcohol use*. PhD thesis, University of Minnesota.

Karpyak, V. M., Biernacka, J. M., Weg, M. W., et al. (2010). Interaction of SLC6A4 and DRD2 polymorphisms is associated with a history of delirium tremens. *Addict. Biol.*, 15:23–34.

Ke, X. (2012). Presence of multiple independent effects in risk loci of common complex human diseases. *Am. J. Hum. Genet.*, 91:185–192.

Keyes, M. A., Malone, S. M., Elkins, I. J., Legrand, L., McGue, M., and Iacono, W. G. (2009). The Enrichment Study of the Minnesota Twin Family Study: Increasing the yield of twin families at high risk for externalizing psychopathology. *Twin Res. Hum. Genet.*, 12:489–501.

Kohler, H. P., Behrman, J. R., and Schnittker, J. (2011). Social science methods for twins data: integrating causality, endowments, and heritability. *Biodemography Soc Biol.*, 57:88–141.

Lamparter, D., Marbach, D., Rueedi, R., et al. (2016). Fast and Rigorous Computation of Gene and Pathway Scores from SNP-Based Summary Statistics. *PLoS Comput. Biol.*, 12:e1004714.

Li, R., Zhong, W., and Zhu, L. (2012). Feature Screening via Distance Correlation Learning. *J. Amer. Statist. Assoc.*, 107:1129–1139.

Li, X., Basu, S., Miller, M. B., Iacono, W. G., and McGue, M. (2011). A Rapid Generalized Least Squares Model for a Genome-Wide Quantitative Trait Association Analysis in Families. *Hum. Hered.*, 71:67–82.

Lind, P. A., Macgregor, S., Heath, A. C., and Madden, P. A. F. (2012). Association between *in vivo* alcohol metabolism and genetic variation in pathways that metabolize the carbon skeleton of ethanol and NADH reoxidation in the Alcohol Challenge Twin Study. *Alcohol Clin. Exp. Res.*, 36:2074–2085.

Macgregor, S., Lind, P. A., Bucholtz, K. K., et al. (2008). Associations of adh and aldh2 gene variation with self report alcohol reactions, consumption and dependence: an integrated analysis. *Hum. Mol. Genet.*, 18:580–593.

Majumdar, S. and Chatterjee, S. (2017). Fast and General Model Selection using Data Depth and Resampling. https://arxiv.org/abs/1706.02429.

Manolio, T. A., Collins, F. S., Cox, N. J., et al. (2009). Finding the missing heritability of complex diseases. *Nature*, 461:747–753.

McGue, M., Keyes, M., Sharma, A., Elkins, I. J., Legrand, L. N., Johnson, W., and Iacono, W. G. (2007). The environments of adopted and non-adopted youth: Evidence on range restriction from the Sibling Interaction and Behavior Study (SIBS). *Behav. Genet.*, 37:449–462.

McGue, M., Zhang, Y., Miller, M. B., et al. (2013). A Genome-Wide Association Study of Behavioral Disinhibition. *Behav Genet.*, 43.

Miller, M. B., Basu, S., Cunningham, J., et al. (2012). The Minnesota Center for Twin and Family Research Genome-Wide Association Study. *Twin Res Hum Genet.*, 15:767–774.

Mosler, K. (2013). Depth statistics. In Becker, C., Fried, R., and Kuhnt, S., editors, *Robustness and Complex Data Structures*, pages 17–34. Springer Berlin Heidelberg.

Rosenbloom, K. R., Armstrong, J., Barber, G. P., et al. (2015). The UCSC Genome Browser database: 2015 update. *Nucleic Acids Res.*, 43:D670–81.

Schaid, D. J., McDonnell, S. K., Sinnwell, J. P., and Thibodeau, S. N. (2013). Multiple Genetic Variant Association Testing by Collapsing and Kernel Methods With Pedigree or Population Structured Data. *Genet. Epidemiol.*, 37:409–418.

Schifano, E. D., Epstein, M. P., Bielak, L. F., Jhun, M. A., Kardia, S. L., Peyser, P. A., and Lin, X. (2012). SNP set association analysis for familial data. *Genet. Epidemiol.*, 36(8):797–810.

Tukey, J. (1975). Mathematics and picturing data. In James, R., editor, *Proceedings of the International Congress on Mathematics*, volume 2, pages 523–531.

Visscher, P. M., Brown, M. A., McCarthy, M. I., and Yang, J. (2012). Five Years of GWAS Discovery. *Am. J. Hum. Genet.*, 90:7–24.

Visscher, P. M., Wray, N. R., Zhang, Q., et al. (2017). 10 Years of GWAS Discovery: Biology, Function, and Translation. *Am. J. Hum. Genet.*, 101(1):5–22.

Voisey, J., Swagell, C. D., Hughes, I. P., et al. (2011). A novel SNP in COMT is associated with alcohol dependence but not opiate or nicotine dependence: a case control study. *Behav. Brain Funct.*, 7(51).

Wang, T. Y., Lee, S. Y., Chen, S. L., et al. (2014). Gender-specific association of the SLC6A4 and DRD2 gene variants in bipolar disorder. *Int. J. Neuropsychopharmacol.*, 17:211–222.

Westfall, P. H. and Young, S. S. (1993). *Resampling-Based Multiple Testing: Examples and Methods for p-Value Adjustment*. Wiley; New York.

Wheeler, E. and Barroso, I. (2011). Genome-wide association studies and type 2 diabetes. *Brief. Funct. Genet.*, 10(2):52–60.

Xu, K., Kranzler, H. R., Sherva, R., Sartor, C. E., et al. (2015). Genomewide Association Study for Maximum Number of Alcoholic Drinks in European Americans and African Americans. *Alcohol Clin. Exp. Res.*, 39:1137–1147.

Yang, J., Ferreira, T., Morris, A. P., et al. (2012). Conditional and joint multiple-SNP analysis of GWAS summary statistics identifies additional variants influencing complex traits. *Nat. Genet.*, 44:369–375 S361–S363.

Zhang, H., Shi, J., Liang, F., et al. (2014). A fast multilocus test with adaptive SNP selection for large-scale genetic-association studies. *Eur. J. Hum. Genet.*, 22:696–701.

Zuo, Y. (2003). Projection-based depth functions and associated medians. *Ann. Statist.*, 31:1460–1490.

Zuo, Y. and Serfling, R. (2000). General notions of statistical depth functions. *Ann. Statist.*, 28-2:461–482.

Appendix

A Proof of theoretical results

Proof of Theorem 3.2. Define $c_{q,\infty} = q^{\text{th}}$ quantile of $\mathbb{T}_0$. Now following assumption (E1),

$$\begin{aligned} c_q(\mathbb{E}_*) &= \inf_\theta \{E(\theta, [\hat{\theta}]) : \mathbb{F}_* \geq q\} \\ &= \inf_\theta \{E(a_n(\theta - \theta_0), [a_n(\hat{\theta} - \theta_0)]) : a_n(\mathbb{F}_* - \theta_0) \geq q\} \end{aligned}$$

where $\mathbb{F}_*$ is the probability distribution function of $E(\hat{\theta}, [\hat{\theta}])$. Part 1 is proved following assumptions (P2) and (E3).

Now if $\mathcal{M}$ is adequate, following assumption (E1),

$$E(\hat{\theta}_m, [\hat{\theta}]) = E(\hat{\theta}_m - \theta_0, [\hat{\theta} - \theta_0]) \tag{A.1}$$

Decompose the first argument as

$$\hat{\theta}_m - \theta = (\hat{\theta}_m - \hat{\theta}) + (\hat{\theta} - \theta_0) \tag{A.2}$$

By definition, $\hat{\theta}_{mj} - \hat{\theta}_j = 0$ if $j \in \mathcal{S}$, else equals $\theta_{0j} - \hat{\theta}_j$. Thus for the first summand in (A.2) we have

$$\hat{\theta}_m - \hat{\theta} = O_P(1/a_n)$$

Going back to (A.1), this implies

$$|E(\hat{\theta}_m - \theta_0, [\hat{\theta} - \theta_0]) - E(\hat{\theta} - \theta_0, [\hat{\theta} - \theta_0])| < O_P(a_n^{-\alpha})$$

using lipschitz continuity in assumption (E2), i.e

$$|E(\hat{\theta}_m, [\hat{\theta}]) - E(\hat{\theta}, [\hat{\theta}])| < O_P(a_n^{-\alpha})$$

again using (E1). Part 2 now follows.

For part 3, we apply (E1) to get

$$E(\hat{\theta}_m, [\hat{\theta}]) = E(a_n(\hat{\theta}_m - \theta_0), [a_n(\hat{\theta} - \theta_0)]) \tag{A.3}$$

And decompose the first argument as

$$a_n(\hat{\theta}_m - \theta_0) = a_n(\hat{\theta}_m - \theta_m) + a_n(\theta_m - \theta_0) \tag{A.4}$$

Since $\mathcal{M}$ is inadequate, $\theta_{mj} \neq \theta_{0j}$ when $j \notin \mathcal{S}$. So $\|a_n(\theta_m - \theta_0)\| \uparrow \infty$ as $a_n \uparrow \infty$. Applying (E4) now proves part 3. □

Proof of Theorem 3.3. The proof is fairly similar to that of theorem 3.2, so we give a sketch of it. For the full model, the bootstrap is consistent, i.e. $a_n(\hat{\theta}_* - \theta_0)$ and $(a_n/\tau_n)(\hat{\theta}_{r*} - \hat{\theta}_*)$ converge to same weak limit in probability, following theorems 2.2 and 2.3 in Majumdar and Chatterjee (2017). Specifically, conditions (A1)-(A6) in Majumdar and Chatterjee (2017) ensure condition (P2) in our paper through theorem 2.2 therein, following which theorem 2.3 ensures that when (A1)-(A6) are satisfied, bootstrap consistency holds. The definition of $\hat{\theta}_m$ now means that $a_n(\hat{\theta}_m - \theta_m)$ and $(a_n/\tau_n)(\hat{\theta}_{rm} - \hat{\theta}_m)$ converge to the same weak limit in probability for any model $\mathcal{M}$. A similar approach as the proof of parts 2 and 3 of theorem 3.2 now follows, with an additional term corresponding to bootstrap estimates in (A.2) and (A.4). □

B Outputs for MCTFR data analysis

Each table gives the 90$^{\text{th}}$ percentile e-values, which are plotted in figures 2, 3, and 4 in main paper, of SNPs analyzed in the gene. Column 'Association' is obtained from the sign of the SNP coefficient in the full model.

SNP name	Location	e-value	Association
rs16859227	46250605	0.89	+
rs572227	46251393	0.13	-
rs534459	46256805	0.24	+
rs2119183	46272806	0.92	-
rs502038	46280318	0.58	+
rs1808851	46311447	0.00	+
rs279856	46317923	0.00	-
rs3775282	46321863	0.86	-
rs279841	46340763	0.75	+
rs10805145	46358331	0.73	-
rs13152740	46381221	0.86	-

Table B.1: SNPs for GABRA2, chr4, position 46243548 - 46390039; e-value cutoff 0.72

SNP name	Location	*e*-value	Association
rs17027299	99078105	0.84	-
rs9307222	99101051	0.76	-
rs10006414	99101401	0.49	+
rs9994641	99101605	0.48	+
rs13134014	99104879	0.75	-
rs6820691	99105055	0.76	+
rs6820913	99125659	0.81	+
rs6532729	99146436	0.67	-
rs13150538	99152631	0.49	-
rs17027380	99157450	0.63	-
rs17494998	99160699	0.41	+
rs549467	99172232	0.81	+
rs2034677	99187874	0.62	+
rs12508445	99190653	0.01	-
rs10003496	99197839	0.81	+
rs10005811	99208603	0.02	+
rs603215	99214851	0.78	-
rs433146	99229839	0.87	-
rs17027456	99235747	0.31	-
rs17561798	99235941	0.85	+
rs10516428	99237439	0.45	-
rs6532731	99251006	0.80	+
rs7694221	99260423	0.90	+
rs10028330	99268949	0.70	-
rs10022047	99296818	0.49	+
rs17027523	99298979	0.05	+
rs17027530	99303633	0.69	+
rs3775540	99304544	0.23	-
rs3756088	99309404	0.89	-
rs13103626	99317251	0.75	+
rs10516430	99337881	0.62	+
rs9884594	99359318	0.68	-
rs12503056	99369061	0.63	+
rs2004316	99381148	0.43	-
rs4303985	99399748	0.87	-
rs4414961	99403784	0.86	-
rs12509267	99407299	0.80	+
rs6838913	99408106	0.84	-
rs4374629	99411783	0.85	+
rs4527483	99421741	0.89	+
rs10009693	99423280	0.90	-
rs10023791	99425353	0.88	+
rs955931	99428163	0.88	-
rs17027628	99428608	0.85	-

Table B.2: SNPs for ADH genes, chr4, position 99070977 - 99435737; *e*-value cutoff 0.225

SNP name	Location	e-value	Association
rs2000371	154011024	0.39	-
rs9371718	154011615	0.08	-
rs12211203	154016936	0.63	-
rs1937600	154017197	0.02	-
rs9397637	154022718	0.00	+
rs1937590	154036895	0.63	+
rs12662873	154040810	0.18	+
rs12661209	154044112	0.84	-
rs1316368	154055754	0.00	-
rs1937587	154060023	0.27	-
rs6921403	154063906	0.00	-
rs1937580	154076643	0.00	+
rs1937645	154082228	0.00	+
rs1892361	154099619	0.00	-
rs1937633	154104857	0.04	-
rs1937631	154105011	0.00	-
rs12527197	154107836	0.02	+
rs1892360	154111701	0.74	-
rs1892359	154112042	0.65	-
rs1892356	154112263	0.56	+
rs1937622	154113139	0.54	-
rs10485258	154113409	0.72	-
rs1937619	154114583	0.58	-
rs1748289	154121980	0.77	-
rs1781619	154135968	0.64	-
rs652051	154139344	0.74	+
rs10485262	154140199	0.69	-
rs9371312	154145492	0.81	+
rs1332849	154151117	0.48	-
rs9371749	154153369	0.28	+
rs9285539	154154532	0.08	+
rs9322439	154156250	0.07	+
rs11752884	154159710	0.25	-
rs4869813	154173845	0.13	+
rs4870241	154174963	0.00	-
rs9384156	154186720	0.13	+
rs2065139	154192175	0.89	-
rs689219	154198820	0.00	-
rs9371761	154202578	0.20	-
rs12199858	154204327	0.00	+
rs9371762	154213973	0.00	-
rs612450	154214357	0.00	-
rs9384159	154219177	0.00	+
rs6938958	154220427	0.00	-
rs581564	154221214	0.00	+
rs12202611	154237443	0.76	-
rs4870255	154237937	0.88	-

SNP name	Location	*e*-value	Association
rs10872828	133525348	0.72	-
rs9419702	133531153	0.09	-
rs7083395	133532269	0.77	+
rs9419624	133534822	0.06	+
rs7906770	133536902	0.28	-
rs9419569	133541881	0.06	+
rs9419629	133543210	0.06	+
rs7093241	133556596	0.72	-
rs9419649	133561098	0.91	-

Table B.4: SNPs for CYP2E1, chr10, position 133520406 - 133561220; *e*-value cutoff 0.72

SNP name	Location	*e*-value	Association
rs7398343	111774068	0.34	-
rs7297186	111778178	0.36	+
rs3803167	111785586	0.00	+
rs10219736	111788402	0.00	-
rs16941437	111793039	0.00	-
rs3742004	111798553	0.75	+

Table B.5: SNPs for ALDH2, chr12, position 111766887 - 111817529; *e*-value cutoff 0.72

SNP name	Location	*e*-value	Association
rs4646312	19948337	0.41	-
rs165656	19948863	0.22	-
rs165722	19949013	0.24	+
rs2239393	19950428	0.50	+
rs4680	19951271	0.60	+
rs4646316	19952132	0.81	-
rs165774	19952561	0.72	-
rs174699	19954458	0.07	+
rs165599	19956781	0.58	-
rs165728	19957023	0.02	-
rs165815	19959473	0.00	+
rs5993891	19959746	0.04	-
rs887199	19961955	0.04	-
rs2239395	19962203	0.07	+
rs2518824	19962963	0.59	+

Table B.6: SNPs for COMT, chr22, position 19941607 - 19969975; *e*-value cutoff 0.72

SNP name	Location	*e*-value	Association
rs27072	1394522	0.87	+
rs40184	1395077	0.78	-
rs11564771	1398797	0.80	-
rs11133767	1401580	0.79	+
rs6869645	1404548	0.82	+
rs3776512	1407116	0.84	+
rs6347	1411412	0.83	-
rs27048	1412645	0.90	-
rs2042449	1416646	0.63	+
rs13161905	1417212	0.72	-
rs2735917	1420268	0.92	+
rs464049	1423905	0.21	-
rs460700	1429969	0.00	-
rs460000	1432825	0.00	+
rs4975646	1433401	0.88	-
rs403636	1438354	0.78	-
rs2617605	1442521	0.89	+
rs6350	1443199	0.93	+

Table B.7: SNPs for SLC6A3, chr5, position 1392790 - 1445430; *e*-value cutoff 0.72

SNP name	Location	*e*-value	Association
rs16967029	30195292	0.79	+
rs2051810	30195841	0.84	-
rs11658318	30206059	0.72	-
rs8079471	30218317	0.64	+
rs3760454	30222002	0.90	+

Table B.8: SNPs for SLC6A4, chr17, position 30194319 - 30236002; *e*-value cutoff 0.63

SNP name	Location	e-value	Association
rs2514229	113410000	0.87	-
rs11214654	113410917	0.86	+
rs7937641	113415976	0.63	-
rs12222458	113417603	0.73	-
rs10736470	113418371	0.73	-
rs12576506	113419869	0.85	+
rs10750025	113424042	0.66	+
rs7952106	113424558	0.70	-
rs4373974	113430486	0.88	-
rs4130345	113436487	0.88	-
rs7123697	113440331	0.78	+
rs6589386	113443753	0.75	+
rs4132966	113451589	0.86	+
rs7940164	113451765	0.90	-
rs4245155	113457324	0.92	-
rs11607834	113461680	0.92	-
rs12280220	113469219	0.93	-

Table B.9: SNPs for DRD2, chr11, position 113409595 - 113475691; e-value cutoff 0.63

C Discussion on gene-specific findings in the MCTFR data

GABRA2: As seen in the plots, the first two SNPs detected are close to two separate exons. The 4th and 5th detected SNPs, rs1808851 and rs279856, are at perfect LD with rs279858 in the larger 7188-individual dataset (Irons, 2012). This SNP had not been genotyped in our sample, but is the marker in GABRA2 that is most frequently associated in the literature with alcohol abuse (Cui et al., 2012). Interestingly, a single SNP RFGLS analysis of the same twin studies data that used Bonferroni correction on marginal p-values to detect SNPs had missed these SNPs (Irons, 2012). This highlights the advantage of our approach.

ADH genes: Multiple studies have associated rs1229984 in the ADH1B gene (position 99318162 of chromosome 4) with alcohol dependence (https://www.snpedia.com/index.php/Rs1229984), which as seen in the plot of ADH2 is close to an exon region. Our data does not contain this marker, but detects one SNP 20 kb upstream of this, rs17027523. Another SNP, rs3775540 at position 99304544 has an e-value of 0.226, so narrowly misses detection. This is close to rs1229984, and also rs1042026 at position 99307309, which Macgregor et al. (2008) found to be strongly associated with alcohol consumption.

The SNP rs17027523 is interesting: it resides in the uncharacterized long non-coding

RNA gene LOC100507053. One previous study (Gelernter et al., 2014; Xu et al., 2015) found significant associations for 5 SNPs in this gene with alcohol consumption for African American population through single-SNP analysis on non-familial GWAS data. Notably, their analysis found a much stronger evidence of the association in African-American part of the sample than the European American part, while our findings are entirely from a Caucasian sample.

OPRM1: Many of the SNPs analyzed in this gene have very low e-values, and tend to cluster together. The minor allele of the SNP rs1799971 (chr 6, position 154039662) has been associated with stronger alcohol cravings (https://www.snpedia.com/index.php/Rs1799971), and we detect rs12662873 at position 154040810.

CYP2E1: Five of the 9 SNPs studied are detected through our analysis. Four of them are within 10 kb of one another (base pairs 133534822 to 133543210 in chr 10). In the analysis of Lind et al. (2012) rs4646976 at 133534223 position was most associated with a measure of breath alcohol concentration: this is within our detected region. This study had also detected rs4838767 in the promoter region of CYP2E1 (position 133520114) associated with multiple alcohol consumption measures. We detect rs9419702 at position 133531153.

ALDH2: All 6 SNPs we study are close to exons, and 5 get picked up by the e-value procedure. While all five are at a lesser base pair position than the well-known SNP rs671 (https://www.snpedia.com/index.php/Rs671, position 111803962), one of the SNPs we analyze (rs16941437) is within 10 kb upstream of this SNP.

COMT: The SNP rs4680 has long been associated with schizophrenia and substance abuse, including alcoholism. A case-control study (Voisey et al., 2011) associated rs4680 and rs165774 with alcohol dependence through a SNP-wise chi-squared test, and had these two SNPs in high LD in their study population. Compared to this, in our simultaneous model of all COMT polymorphisms, the more well-known rs4680 has a below threshold e-value.

SLC6A3: Our analysis does not detect rs27072, which has been associated with alcohol withdrawal symptoms (https://www.snpedia.com/index.php/Rs27072).

Finally, most e-values for the last 3 genes, i.e. SLC6A3, SLC6A4 and DRD2, are large: indicating weak SNP signals. We found this observation interesting, because variants of these genes have known interaction effects behind alcohol withdrawal-induced seizure (Karpyak et al., 2010) and bipolar disorder (Wang et al., 2014), as well as additive effect on the susceptibility to smoking addiction (Erblich et al., 2005).